Environ Earth Sci (2016) 75:860
DOI 10.1007/s12665-016-5596-3

ORIGINAL ARTICLE

Empirical rock mechanical site-descriptive modeling (RMSDM) for the Korea Atomic Energy Research Institute Underground Research Tunnel (KURT)

Qing-Zhao Zhang[1,3] · Hyun-Sic Jang[1] · Dae-Seok Bae[2] · Geon-Young Kim[2] · Bo-An Jang[1]

Received: 3 August 2015 / Accepted: 28 March 2016 / Published online: 10 May 2016

Abstract As part of master plan, when preparing to construct the second stage of the Korea Atomic Energy Research Institute Underground Research Tunnel (KURT-2), site investigations were carried out to characterize the rock mass and its related geophysical nature. The rock mass at the study site was divided into rock units depending on a rock type and fracture developments in rock. The rock mass quality for each rock unit was evaluated, using rock mass classification systems, such as Q, rock mass rating (RMR), and rock mass index (RMi). The mechanical properties of rock units were empirically estimated with associated rock mass classification systems, including deformation modulus, uniaxial compressive strength, and cohesion and friction angles. Ultimately, a rock mechanical site-descriptive model (RMSDM) covering the block size of 85 m × 120 m × 80 m was developed by combining the analysis of rock units. Rock block consists of granite, dike, and fault, being divided into six rock units, such as G1, G2, G3, D1, D3, and F3. G1 and D1 rock units were classified as good rock masses, and the rock mass quality of G2 is fair. G3 and D3 rock units were classified as poor rock masses, and the F3 rock unit was very poor. The mechanical properties of rock unit G1 and D1 were almost considered similar and best, and those of G2 were considered middle class. G3 and D3 rock units had poor mechanical properties and those of F3 were the worst. G1 occupies most of block volume, but other rock units were distributed as small portions. Two-dimensional distributions of rock mass from modeling and face mapping at the elevation of the tunnel excavation exhibited that predicted distributions well fit to those observed. Therefore, RMSDM will be of help with the geoscientific understanding of site investigation and designing of a site and construction of a site, similar to KURT-2, and ultimately, it will become a scientific base to future-related research and development projects of the Korea Atomic Energy Research Institute (KAERI).

Keywords Korea Atomic Energy Research Institute Underground Research Tunnel (KURT) · Rock unit · Rock mass classification · Rock mechanical site-descriptive model (RMSDM) · Safe disposal of spent nuclear fuel (SNF)

✉ Bo-An Jang
bajang@kangwon.ac.kr

[1] Department of Geophysics, Kangwon National University, Chuncheon, Gangwon-do, Republic of Korea

[2] Korea Atomic Energy Research Institute, Yuseong, Daejeon, Republic of Korea

[3] Department of Geotechnical Engineering, College of Civil Engineering, Tongji University, Shanghai 200092, China

Introduction

Deep geological disposal is regarded as the most reasonable and effective method for the safe disposal of spent nuclear fuel (SNF), and has been widely investigated worldwide (Andersson et al. 2013). Many countries have constructed and operated several types of underground research facilities to evaluate the feasibility, safety, and technical performance of their SNF disposal systems (Bredehoeft 2005; Nordstrom 2012). In 2006, the Korea Atomic Energy Research Institute (KAERI) proposed a conceptual design of geological disposal system for SNF in Korea (Cho et al. 2008). This concept was established based on a representative geological data set from granites, which were regarded as one of the preferable host rocks

(Kwon et al. 2009). During the early stages in the national research and development program for SNF disposal in Korea, KAERI constructed a small-scale underground research tunnel termed the KAERI Underground Research Tunnel (KURT) to improve research technology, obtain experience, and eventually build an optimum system. The construction of KURT-1 (the first stage of KURT) was completed by a controlled blasting technique in 2006 (Kwon et al. 2004). KAERI is currently constructing the second stage of KURT (KURT-2) to conduct future research programs.

For deep geological repositories, site geoscientific models were prepared and updated during site investigations. A site-descriptive model was vital for understanding investigated sites and its numerous data. It will form a basis for subsequent repository design planning and safety assessment studies. This led to a modeling study for verification on the data from site investigation. New model versions were prepared as new information became available (SKB 2000). The rock mechanical site-descriptive model (RMSDM) is one of the several site-descriptive models that will constitute geology, rock mechanics, thermal properties, hydrogeology, hydrogeochemistry, transport properties, and surface ecosystems, etc (SKB 2002). The RMSDM was known for a site characterization (Makurat et al. 2006).

Rock mass classification is an essential element for building an RMSDM. Various classification systems were developed to estimate tunnel support loads and characterize mechanical rock mass properties. Many classification systems, such as rock structure rating (RSR), rock mass rating (RMR), rock mass strength (RMS), and rock mass quality system (Q-system), were suggested after Terzaghi's rock load theory (Barton 1988; Bieniawski 1973, 1976; Grimstad and Barton 1993; Terzaghi 1946). Such systems were based on many case studies of underground excavation stability, mainly pertaining hard rock (Barton et al. 1974). Later, additional classification systems were developed, such as rock mass index (RMi) classification system, based on a jointing parameter and intact rock strength. This was more based on a geological strength index (Hoek 1994; Hoek et al. 1995; Palmström 1995, 1996). The mechanical properties of rock mass, including deformation modulus, compressive strength, cohesion, and friction angles, are also significant factors to the RMSDM, because they are of great importance in designing engineering structures and mathematical calculation.

The RMSDM should provide a reliable description of the distribution of rock mass quality and the mechanical properties of a site area. The model will describe constructability, risk estimation for stability problems, and assessment of rock support needs (Brantberger et al. 2006; SKB 2000, 2001). It can describe the safety assessment from an analysis of thermo-mechanically induced changes in the repository near field with seismically induced slip on fractures (Fälth and Hökmark 2006). The strategy for the RMSDM content and its development was described from theoretical, empirical, and numerical aspects in some literatures (Andersson et al. 2002; Hakami et al. 2002; Hudson 2002; SKB 2002; Staub et al. 2002). The modeling methodology was also evaluated in specific cases at the Forsmark site and the Aspö Hard Rock Laboratory in Sweden, and in a circular tunnel through the Yucca Mountain in the United States of America (Glamheden et al. 2007; Hashemi et al. 2010; Holland and Lorig 1997; Makurat et al. 2006; Rönkkönen et al. 2012; SKB 2001). However, interpretations of rock mass for the development of an RMSDM are site-dependent and require further studies for many different sites.

This study describes a case study for the building of an RMSDM for expanded KURT-2 construction using an empirical approach. The modeling strategy consists of analyzing rock quality with regard to site characteristics and tunneling works, and evaluating the distribution of basic rock mechanical properties, such as deformation and strength properties. Data obtained from site investigations were evaluated, and rock mass qualities were characterized using rock mass classification systems. Preliminary data used for the modeling work were obtained mainly from measurements of geological and mechanical rock mass properties during the site investigations. However, given that some mechanical properties were difficult to directly measure because of certain limitations and borehole conditions at the site, they were estimated from relationships with rock mass classification. Although an estimation of mechanical parameters using classification systems was investigated by numerous researchers and specifically utilized for many projects (Barton 2008; Bieniawski 1978; Hoek and Brown 1980; Mehrotra 1992; Mitri et al. 1994; Palmström and Singh 2001; Ramamurthy 1986; Read et al. 1999; Sonmez et al. 2006), their applicability to rock masses in this study still needs to be extensively tested, and technically verified in a way. Finally, a three-dimensional RMSDM was established using the distributions of rock units and mechanical properties in each rock unit and compared with the post excavation.

Materials and methods

Site geology

KURT was constructed in Daejeon, which is located near the middle of South Korea and approximately 150-km south bound of Seoul, the Metropolitan Capital City (Fig. 1). It is located in a mountain adjacent to the KAERI site with its

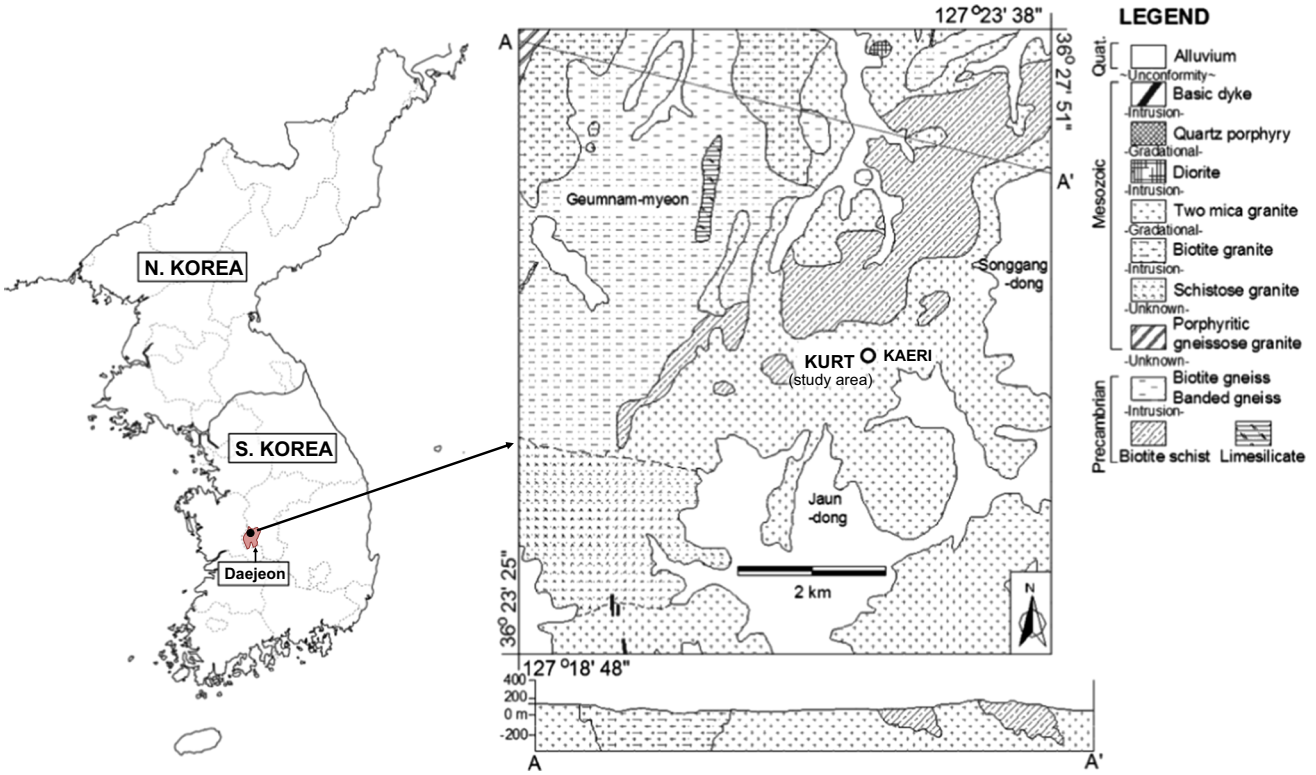

Fig. 1 Location and geological map of KURT area (After Kim et al. 2012)

portal on a hillside approximately 110 m above the sea level. A previous geological survey was conducted at the study area during the KURT-1 construction. The dominant rock type in the study area is granite, but andesite dikes appear at some locations. A weathered residual soil layer from the granitic host rock covers the ground surface. A weathered and weak rock layers are distributed underneath weathered soil layer. The total thickness of soil, weathered rock, and weak rock layers is approximately 40 m from the surface (Kwon and Cho 2008). KURT-1 is 255-m long with a 180-m-long access tunnel and two research modules with a total length of 75 m (Kwon and Cho 2009). Its horseshoe-shaped cross section is 6 m wide and 6 m high. A 10 % downward slope and tunnel direction toward the top of the mountain was chosen because of better rock mass quality (Kwon et al. 2004). KURT-2 begins at the end of the access tunnel in KURT-1 and has more complicated layout than KURT-1 does. Mesozoic two-mica granite is the major rock type and is distributed widely. Numerous dikes exist in the granitic rock body. Precambrian biotite gneiss and schist are distributed 1–3 km around the study area. During the previous geological investigation, it was found that the rock mass quality improved with depth (Kwon et al. 2004). A simplified geological map of the KURT area is shown in Fig. 1.

Site investigations

Site investigations are a comprehensive task to understand rock formations from surface and borehole data. The main purpose of a site investigation was to characterize the geology of the study area and rock mechanics of the rock formation. Local in situ structural geology data, rock types, and fractures provide a basis for the conceptual idea of structural geology at the site. Rock mechanical data of different rock types from borehole measurements and laboratory tests provide a basis for the distribution pattern of basic rock mechanical properties. A surface survey, borehole logging, televiewer imaging, and laboratory tests were also carried out to investigate geological characteristics and rock mechanical properties. Borehole logging was the main approach as well as data source for the collection of information, such as RQD and lithology. The joint condition was studied from drill cores and the televiewer image of boreholes. Fracture parameters like roughness, weathering, infilling, and aperture were obtained from borehole loggings, too. Borehole data were obtained from three deep boreholes, such as KP-1, KP-3, and KP-4, with a total length of 270.8 m. KP-1 was drilled in N56 W at 5.7° downward with a length of 252.3 m, but only the latter, 83.3 m covered the KURT-2 domain. The other two boreholes, KP-3 and KP-4,

were drilled from the end of the KURT-1. KP-3 was drilled in N82 W at 30° downward with a length of 86.5 m. The orientation of KP-4 was in N10 W with a dip of 30° and the drilling length of 101.0 m.

Modeling procedure

An RMSDM should provide three-dimensional rock unit geometry and characteristics (Hudson 2002). The rock masses along the boreholes can be classified as rock units depending on the rock types, and each rock unit can be subdivided by geological structures. Lithology, rock quality designation (RQD), and fault zones can also be applied as key factors in rock unit classification. The three-dimensional rock mass geometry can be established by identifying and combining the same rock units. Rock mass qualities of rock units can be classified using several rock mass classification systems, such as the Q-system, RMR, and RMi. Rock unit mechanical properties, including the modulus of deformation, strength, friction angle, and cohesion of rock units can be estimated using empirical relationships with such rock mass classification systems.

Rock mass classification systems

Among many rock mass classification systems, the Q-system and RMR are the most widely used for rock engineering applications. The Q-system is based on six parameters (Eq. 1) and its value ranges from 0.001 to 1000 (Barton et al. 1974).

$$\mathrm{Q} = \frac{\mathrm{RQD}}{J_\mathrm{n}} \times \frac{J_\mathrm{r}}{J_\mathrm{a}} \times \frac{J_\mathrm{W}}{\mathrm{SRF}}, \tag{1}$$

where J_n is the joint set number, J_r is the joint roughness number, J_a is the joint alteration number, J_w is the joint water reduction factor, and *SRF* is the stress reduction factor.

The RMR was developed by the South African Council of Scientific and Industrial Research (Bieniawski 1973). It also uses six parameters: the uniaxial compressive strength of intact rock, RQD, the spacing of joints, the conditions of joints, groundwater conditions, and the orientation of joints. The RMR value is obtained by adding the ratings of the six parameters. More recently, the RMi was suggested by Palmström (1995) to represent the rock mass strength. It can be calculated by combining the uniaxial compressive strength (UCS) of intact rock and a jointing parameter J_P (Eq. 2).

$$\mathrm{RMi} = \sigma_\mathrm{ci} \cdot J_\mathrm{p}, \tag{2}$$

where σ_ci is the UCS of intact rock, J_p is the reduction factor representing the block size, and the condition of its surfaces as represented by the friction properties.

The jointing parameter is given by:

$$J_\mathrm{p} = 0.2j\mathrm{C}^{0.5}V_b^D, \tag{3}$$

where V_b is the block volume in m^3 and jC is the joint condition factor expressed as:

$$j\mathrm{C} = j\mathrm{L}(j\mathrm{R}/j\mathrm{A}) \tag{4}$$

$$D = 0.37j\mathrm{C}^{0.2}, \tag{5}$$

where jL is the joint length and continuity factor, jR is the joint wall roughness, and jA is the joint wall alteration factor.

Each classification system consists of various parameters. Some parameters are common, but others are not. The Q-system and the RMR partly use the same parameters. Joint conditions (e.g., roughness, weathering, in-filling, aperture, and groundwater) are used in both the systems. jA and jR used in the RMi are similar to J_r and J_a in the Q-system, respectively.

Rock quality designation (RQD)

RQD has been widely used in rock classification because of its relative simplicity and usable classification of rock mass (Zhang and Einstein 2004). RQD values were calculated directly from borehole logging records (Fig. 2). The average RQD values for KP-1, KP-3, and KP-4 were 71.2, 74.0, and 73.8 %, respectively. However, relatively low RQD values less than 20 % were identified at two or three zones in each borehole. As for KP-1, a RQD less than 20 % was found in a zone between 177.0 and 183.0 m. Zones between 4.4 and 6.9, 8.9–13.3, and 77.0–84.0 m in KP-3, and 30.6–33.3 and 89.8–94.4 m in KP-4 had an RQD less than 20 %. Fault zones with fault breccia and highly weathered calcite were observed in low RQD zones at relatively shallow depths. The low RQD values in deep zones were attributed to severe fracture development. The rock quality was classified into five groups by RQD (Deere 1968). Although most of the rock mass was excellent quality, rock mass near the fault zones was poor quality. Rock masses at the fracture zone were also poor quality.

Uniaxial compressive strength (UCS)

The UCS was measured from intact cores sampled at constant interval along the boreholes, except for KP-1, where measurements were taken during the construction of KURT-1 (Kwon et al. 2004, 2006). A servo-controlled compression device, manufactured by Kyungdo Testing Machine Co. Ltd. in Korea, was used for the uniaxial compression tests. The maximum compressive load for the vertical axis was 2000 kN. UCS values for KP-3 and KP-4 were measured by uniaxial compression and point load

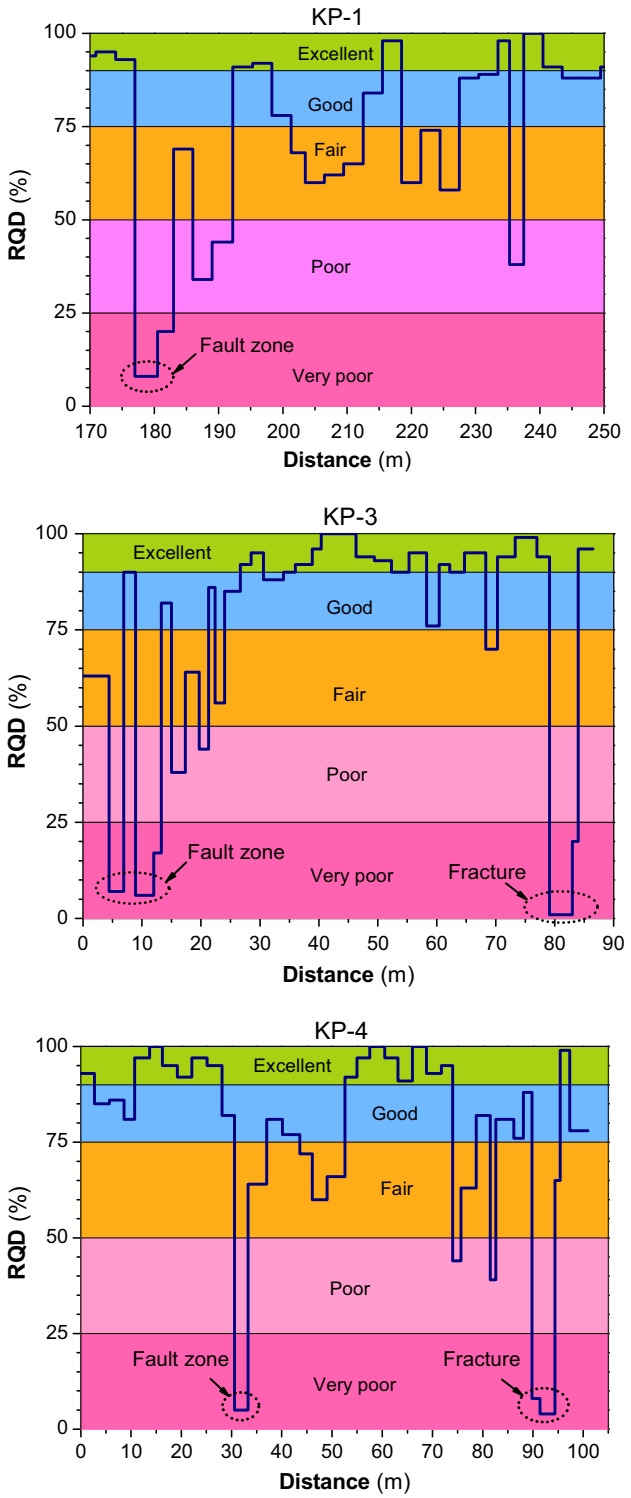

Fig. 2 Distributions of RQD along boreholes, rock qualities as five groups

tests. Figure 3 shows the UCS distributions along KP-3 and KP-4, which varied from 25.0 to 232.8 MPa at the KURT-2 site, with an average of 116.8 and 119.2 MPa for KP-3 and KP-4, respectively. Most samples had a UCS greater

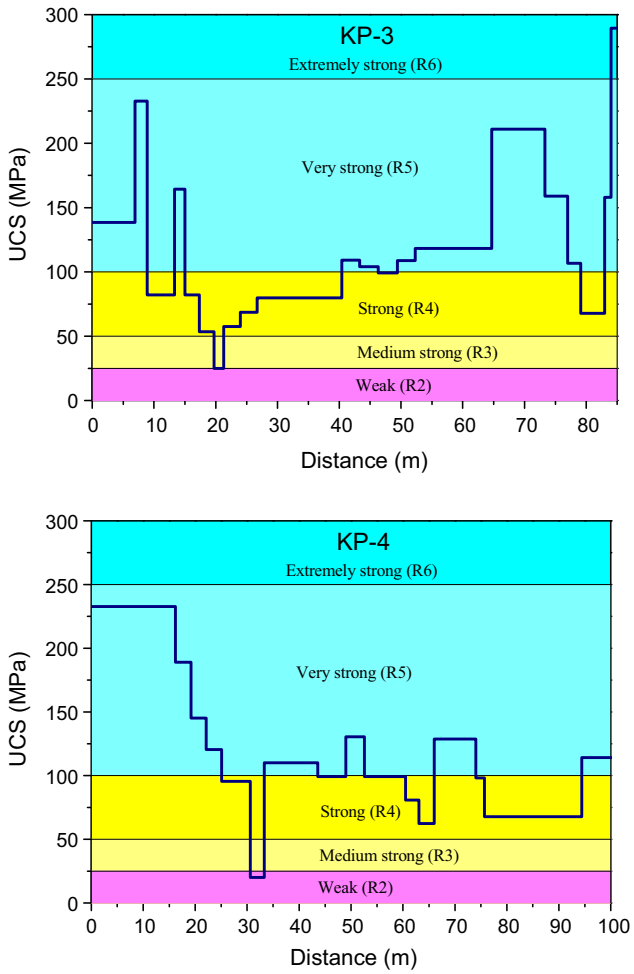

Fig. 3 Distributions of UCS along KP-3 and KP-4 boreholes, rock qualities as five zones

than 100.0 MPa, which could be regarded as high in strength (Ramamurthy and Arora 1993). Boreholes were divided into five zones based on a rock strength classification system suggested by the International Society for Rock Mechanics (ISRM 1981). Most UCS values were distributed in strong (R4) and very strong (R5) zones. In particular, UCS values higher than 250.0 MPa (R6) were found at 84.0–86.5 m for KP-3, while a UCS value of less than 50.0 MPa is at between 19.7 and 21.3 m for KP-3 and 30.6–33.3 m for KP-4.

Results and discussion

Divisions of rock units

Rock mass can be divided into several rock units depending on rock type, so that codes can be assigned to each rock unit. The same code can be used for the same rock type, regardless of the degree of alteration. Granite was the main

rock type in the study area and was assigned the letter (G). Fault zones (F), and dikes (D) were treated as independent rock units. Figure 4a shows the distribution of rock units by rock types along boreholes. Granite was dominant in the domain along the boreholes. Fault zones appeared between 177.0 and 180.5 m for KP-1, 8.9–13.3 m for KP-3, and 30.6–33.3 m for KP-4. Fault-zone thicknesses were less than 5.2 m. Dikes existed mainly in the deeper domains of KP-1 and KP-3 with a thickness of more than 10.0 m. However, dikes in KP-4 were distributed out sporadically with thinner widths.

Rock mass can be divided into three rock units depending on RQD in Fig. 4b (Deere 1968). Zones with a RQD higher than 75 % were classified as a good rock unit with the value 1. Zones with a RQD between 50 and 75 % and those less than 50 % were termed fair and poor rock units, with the assigned values of 2 and 3 for each rock unit (Fig. 4b). In KP-3, a very high 2.0-m-thick RQD zone was identified between two zones with a very low RQD (Fig. 2). This zone was included with the poor zone. Good, fair, and poor rock units occupied 52–76.3, 15.1–25.8, and 7.3–22.2 % of the zone, respectively. The sequences of rock unit distributions were similar along the three boreholes, although their thicknesses differ. Rock units with the same codes were therefore connected.

Rock units classified by rock types were divided into more detailed units using rock units divided by RQD (Fig. 4c). Six different rock units were identified, and a code was assigned for each unit. Granite was divided into three rock units, G1, G2, and G3, which represented granite with good, fair, and poor RQD, respectively. Dikes were divided into two units, D1 and D3. Dikes with a fair RQD were not included in this domain. The RQD in a fault zone was low. All fault zones were represented by F3, a rock unit with poor RQD. To visualize the characteristics of the rock mass at the KURT-2 domain, three-dimensional distributions of rock units along boreholes and its layout of KURT-2 are shown in Fig. 5.

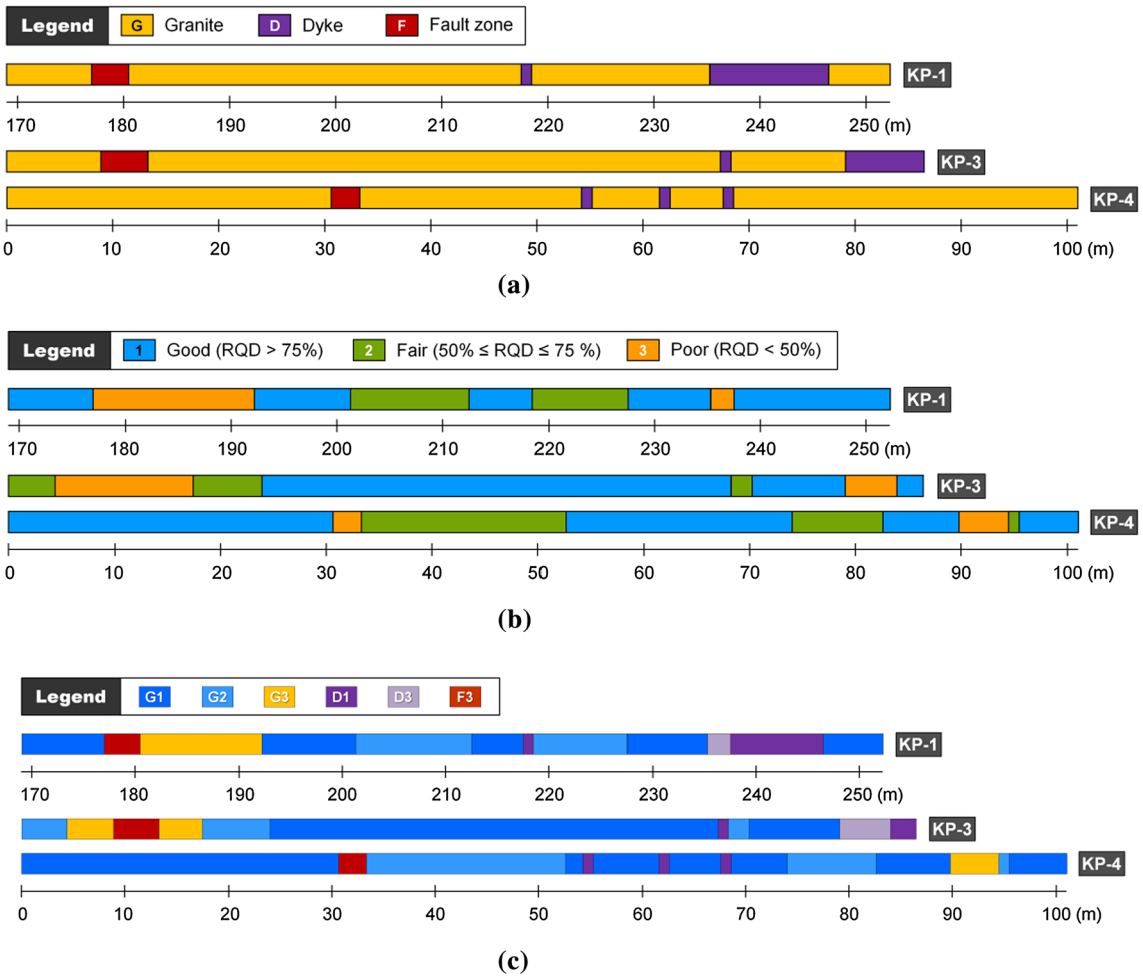

Fig. 4 Rock units division based on lithology and RQD. **a** rock units grouped by lithology along boreholes, **b** rock units grouped by RQD along boreholes, and **c** final rock units grouped by lithology and RQD along boreholes

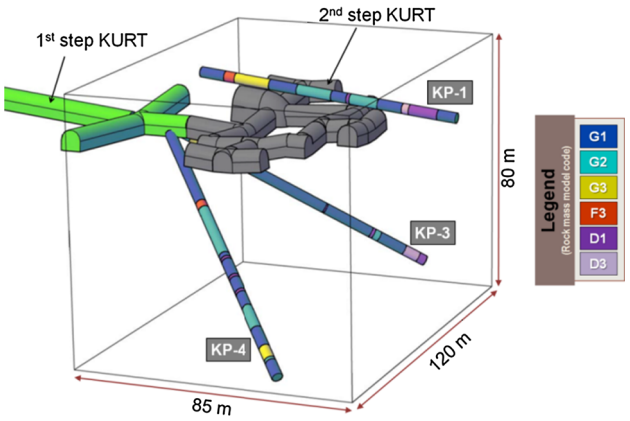

Fig. 5 Three-dimensional distributions of KURT-2 tunnel layout and boreholes with rock units

Rock mass qualities

The Q values of rock mass along each borehole were calculated (Fig. 6). Q values were measured within each drilling interval which was the same as RQD measurements. J_n, J_r, and J_a were obtained from the borehole logging data. Water inflow was medium along most of borehole, but large inflow was recorded in the fault zone. Thus, J_w was set as 0.66, except for fault zones where J_w was equal to 0.5 (Makurat et al. 2006). Because, the study area belongs to the area of medium stress and favorable stress condition; *SRF* was assumed to be 1.0.

Although the rock mass was usually classified into nine classes based on Q values (Singh and Goel 2011), the rock mass along boreholes in this study was divided into six classes. The poor class was sub-divided to exceptionally poor and extremely poor, and the exceptionally good category was included for the extremely good class. Most Q values ranged from 4.0 to 40.0 were the fair and good classes, respectively. Very few portions were included for the extremely good and very poor classes. The distributions of rock units along the boreholes were shown at the bottom of the figures. The Q values of the G1 unit were the good and very good classes, while those of G2 were from fair to poor. The G3 and F3 units were in for poor to very poor classes. The maximum, minimum, and average Q values are listed in Table 1. G1 and D1 showed the highest average Q values of 28.4 and 34.3, respectively, belonging to good rock masses. The Q values of G3 and D3 were lower than 3.0, and such units were classified poor rock mass. F3 had the lowest Q value as very poor rock mass.

RMR values along boreholes are also shown in Fig. 7. They were calculated within each drilling interval which was as same as for Q by method. Most parameters for RMR, such as strength of intact rock, RQD, spacing, and condition of discontinuities, were obtained from the borehole logging data. However, the groundwater conditions and the joint orientation effect from tunnel excavation could not be measured. Therefore, the groundwater condition was assumed to be seven, and the joint orientation effect was not included in the calculation of RMR. This meant for the RMR values were RMR_{basic}.

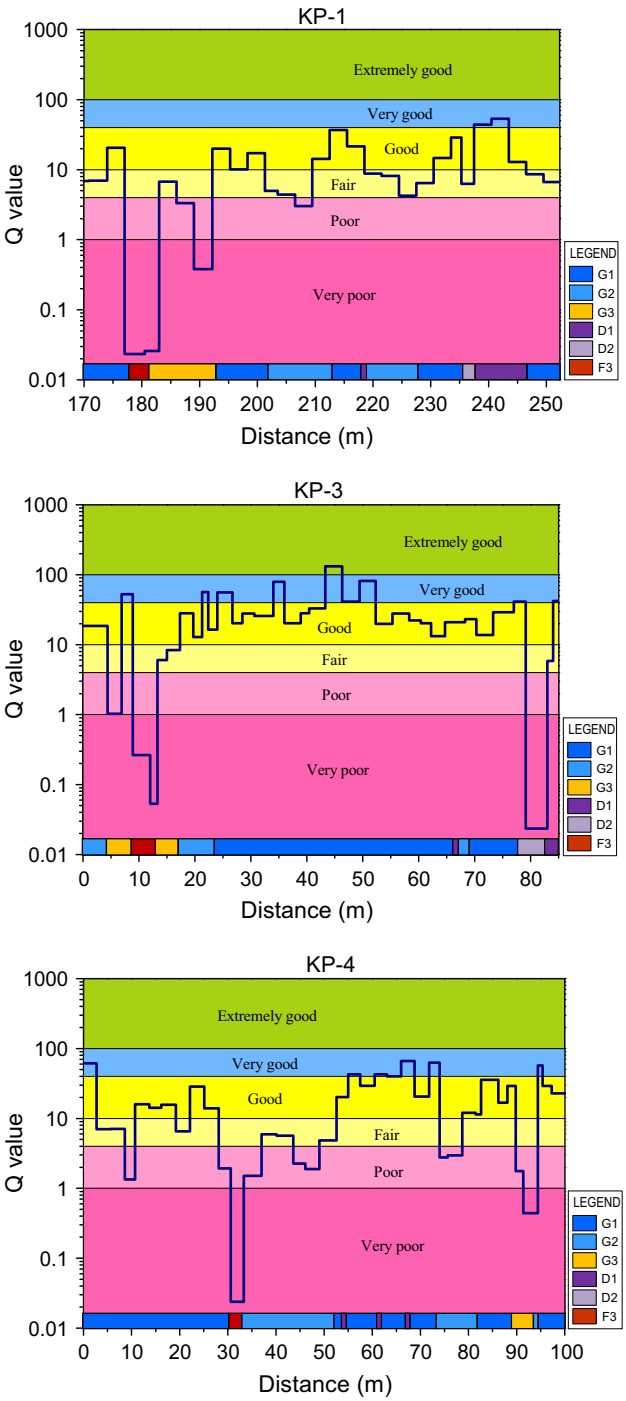

Fig. 6 Distributions in Q value and rock quality classifications along boreholes, rock units along borehole

Table 1 Q-values, RMR, and RMi of rock units along the boreholes

	Code	Average	Max.	Min.	St. dev.	CV (%)
Q value	G1	28.4	132.0	1.3	23.6	83
	G2	9.80	57.2	1.0	11.0	112
	G3	3.00	8.40	0.0	3.20	105
	D1	34.3	66.0	5.9	17.0	50
	D3	2.10	6.30	0.0	3.20	153
	F3	0.10	0.30	0.0	0.10	116
RMR	G1	64.1	73.4	48.0	4.5	7
	G2	52.5	65.6	40.7	5.8	11
	G3	43.5	50.4	33.4	6.2	14
	D1	61.8	71.1	50.3	7.6	12
	D3	39.7	45.0	37.1	4.1	10
	F3	29.3	39.7	21.6	7.4	25
RMi (MPa)	G1	17.7	45.2	1.7	9.80	55
	G2	5.80	23.1	1.3	4.30	74
	G3	3.70	9.00	0.1	3.10	82
	D1	33.6	48.8	5.8	14.5	43
	D3	2.20	5.00	0.8	2.20	101
	F3	0.50	1.50	0.1	0.70	139

CV coefficient of variation, defined as the ratio of standard deviation to mean value

Although rock masses were divided into five classes depending on RMR values (Bieniawski 1973), only three classes (e.g., good-to-poor rock mass), were distributed in the domain. Most rock masses along three boreholes were good or fair, and only few portions were belonging to poor rock masses. Rock masses of the G1 and D1 units were mostly good, but the G2 unit was in the fair class. Rock masses of the G3 and D3 units ranged from fair to poor. F3 had the lowest RMR values and was belonging to the poor class. The average RMR values for rock units are presented in Table 1. The G1 and D1 units had average RMR values of approximately 64.1, which were deemed in the lower part of the good rock mass. G2 and G3 were 52.5 and 43.5, respectively, which were deemed in the fair rock mass range. The average RMR value for D3 was 39.7, which existed on the border between fair and poor rock masses. The average RMR value for F3 was 29.3. The differences in RMR values between the best and worst rock unit were smaller than those for the Q-system. This was because RMR was calculated on a linear scale, whereas Q was on a logarithmic scale.

RMi was so effective as to characterize rock mass strength (Palmström 1995). RMi values along three boreholes are shown in Fig. 8. Palmström (1995) classified rock mass into seven classes from extremely strong to extremely weak, but only four classes were distributed in the study area. The majority of rock mass had RMi values above

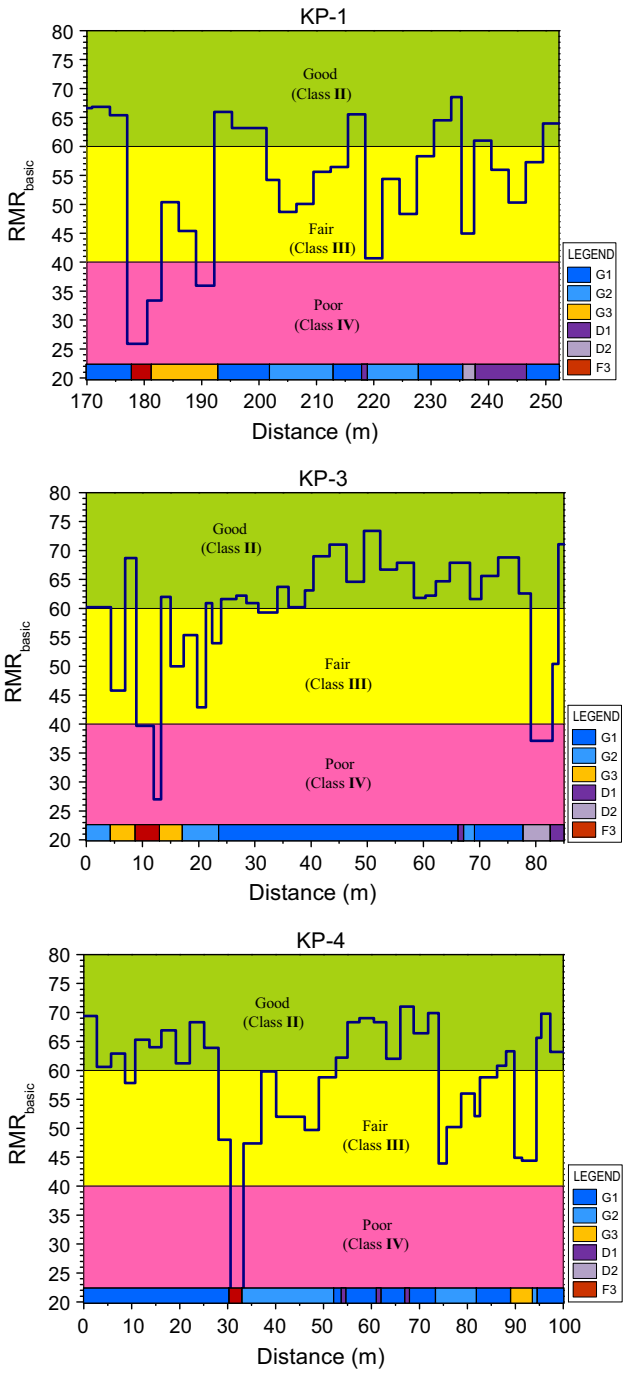

Fig. 7 Distributions in RMR and rock quality classifications along boreholes, rock units along borehole

1.0 MPa, which indicated a strong and very strong class. The G1 and D1 units were belonging to very strong classes, which was the same behavior as the RMR and the Q-system. The G2 unit was classified as strong class. The G3 and D3 units were in the strong classes, which was slightly different from the other classification systems. The F3 unit was in the weak class. The average RMi values calculated

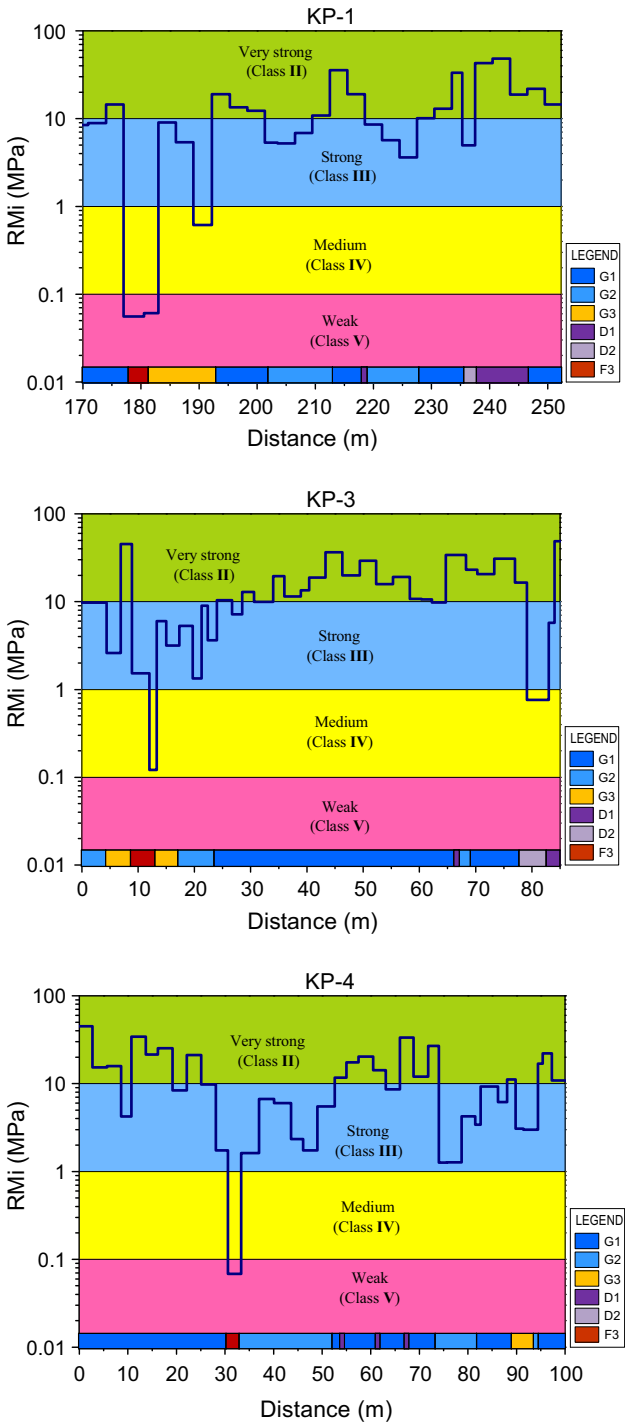

Fig. 8 Distributions of RMi and rock quality classifications along boreholes, rock units along borehole

for the rock units are shown in Table 1. The G1 and D1 rock units had an RMi of 17.7 and 33.6 MPa, respectively, which means for a very strong rock mass. Unlike the other classification systems, the RMi value of D1 was much higher than that of G1. The average RMi values of the G2, G3, and D3 units were between 1.0 and 10.0 MPa, which indicates that rock masses of these units were strong. The RMi classified the F3 as "medium" rock mass. Compared with the RMR and the Q-systems, RMi was likely to give a relatively high evaluation for the rock mass classification.

Deformation modulus

Deformation modulus, E_m, is the most representative mechanical parameter of rock mass. Because, in situ tests usually require a considerable cost and time (Chun et al. 2006); many researchers predict E_m using the empirical rock mass classification systems. Various empirical systems were suggested (Table 2). Equations proposed by Bieniawski (1978), Mehrotra (1992), Read et al. (1999), Chun et al. (2006), Kim and Kim (2006), and Kang et al. (2013) used RMR, whereas the Q-system was used in equations by Grimstad and Barton (1993), Barton (2000), and Kang et al. (2013). Nicholson and Bieniawski (1990), Mitri et al. (1994), and Sonmez et al. (2006) used the elastic modulus of intact rock and RMR, and the equations by Palmström (1996) and Palmström and Singh (2001) used RMi.

E_m values empirically estimated were dependent on the values of the rock mass classification systems, which varied along the borehole and within each rock unit (Figs. 6, 7, 8). In Fig. 7, the RMR value was constant during some borehole intervals, but differed for the next interval. The RMR value in each interval and the interval lengths were collected for each rock unit, and the E_m of each interval was calculated using the equational relationships in Table 2. The distribution of E_m values was divided into several groups at 5 MPa intervals and the total length of each group was measured. The same sequence was applied for the Q-system and the RMi.

Figure 9 shows the histograms of E_m distribution against length and normal distribution curves for the rock unit G1. The distributions of E_m calculated for G1 showed that the relationships proposed by Nicholson and Bieniawski (1990), and Mitri et al. (1994) estimated the high values of E_m, whereas those proposed by Mehrotra (1992), Palmström (1996), Kim and Kim (2006), Chun et al. (2006), and Kang et al. (2013) provided relatively low values (Fig. 9a). Relationships proposed by Bieniawski (1978), Grimstad and Barton (1993), Read et al. (1999), Palmström and Singh (2001), Barton (2000, 2008), Kim and Kim (2006) resulted in medium and similar values. Histograms of E_m from such relationships are shown in Fig. 9b, and E_m values in G1 were estimated using such relationships. The distributions of E_m calculated for G2 and D1 showed almost the same pattern as G1, so E_m values were assessed using the same relationship for G1.

The same approach as above was applied to evaluate the E_m distribution for the rock unit G3, using relationships in

Table 2 Relationships to estimate deformation modulus E_m

Empirical equation	Required parameters	Equations
Bieniawski (1978)	RMR	$E_m = 2\text{RMR} - 100 (\text{RMR} > 50)$
Nicholson and Bieniawski (1990)	RMR, E_i	$E_m = E_i/[100(0.0028\text{RMR}^2 + 0.9e^{\text{RMR}/22.82})]$
Mehrotra (1992)	RMR	$E_m = 10^{(\text{RMR}-20)/38}$
Grimstad and Barton (1993)	Q	$E_m = 25 \log Q$
Mitri et al. (1994)	RMR, E_i	$E_m = E_i\left[0.5\left(1 - \cos\left(\pi\text{RMR}/100\right)\right)\right]$
Palmström (1996)	RMi	$E_m = 5.6\text{RMi}^{0.375}$
Read et al. (1999)	RMR	$E_m = 0.1\left(\text{RMR}/10\right)^3$
Palmström and Singh (2001)	RMi	$E_m = 7\text{RMi}^{0.4}$
Barton (2000)	Q_c	$E_m = 10Q_c^{1/3}\ Q_c = Q\sigma_{ci}/100$
Chun et al. (2006)	RMR	$E_m = 0.3228e^{(0.0485\text{RMR})}$
Kim (1993)	RMR′	$E_m = 300e^{0.07\text{RMR}'} \times 10^{-3}$
Sonmez et al. (2006)	RMR, E_i	$E_m = E_i \times 10^{\frac{(RMR-100)(100-RMR)}{4000e^{(-RMR}/100)}}$
Barton (2008)	Q, q_c	$E_m = 10\left(Qq_c/100\right)^{1/3}$
Kang et al. (2013)	RMR	$E_m = 10^{0.0185\text{RMR}-0.322}$
Kang et al. (2013)	Q	$E_m = 10^{0.32\log Q\ +\ 0.585}$

σ_{ci}, q_c UCS of intact rock, Q_c Q normalized by $\sigma_{ci}/100$, E_i elastic modulus of intact rock, RMR' RMR without ground water and joint orientation factors

Table 2. Some relationships resulted in low values of E_m, whereas E_m values were high in the other equations. The relationships suggested by Palmström (1996), Read et al. (1999), Palmström and Singh (2001), Barton (2000, 2008), Kim and Kim (2006) provided medium values of E_m, thus estimating the E_m of G3. The E_m for the rock units D3 and F3 were also assessed using the same relationship.

Five relationships, such as Read et al. (1999), Palmström and Singh (2001), Barton (2000, 2008), Kim and Kim (2006) used good rock units and poor rock units, whereas those suggested by Bieniawski (1978) and Grimstad and Barton (1993) were only applicable to good rock units and that proposed by Palmström (1996) was applicable only to poor rock units. The reason was all the relationships listed in Table 2 were suggested based on site-specific investigations. In other words, the results derived from this study might be very specific to this site and not to different sites.

Means, standard deviations, and coefficients of variations of E_m for rock units are summarized in Table 3. The E_m of G1 and D1 were the highest and almost same at approximately 30.0 GPa. G2 had medium values of 16.1 GPa. E_m of G3, D3, and F3, poor rock units, were the lowest with less than 10.0 GPa. The deformation modulus derived from empirical relationships should be verified by in situ experiments. However, in situ experiments were not included in the scope of the site investigation.

Compressive strength

The compressive strength is a very important factor for the safe design and engineering, and the construction of tunnels. Compressive strength of small-scale intact rock can be easily measured by the laboratory test. However, its measurement for the large-scale rock mass in field is somewhat difficult, even expensive, and time-consuming. Therefore, the compressive strength of the rock mass is commonly estimated by the rock mass classification and the strength of intact rock. Many empirical relationships have been suggested (Table 4). Most relationships used the RMR and the UCS of intact rock, but some relationships used only the RMR or the UCS of intact rock. Relationships that used the Q-system were also proposed.

The same method as used for the determination of deformation modulus was applied to estimate the compressive strength of the rock mass. Five equations proposed by Hoek and Brown (1980), Ramamurthy (1986), Sheorey (1997), Trueman (1988), and Barton (2000) were selected to identify the compressive rock mass strength for both good and poor rock units, but the equation suggested by Barton (2000) was used only for poor rock units.

The rock mass strengths estimated from the relationships and the RMi for rock units are listed in Table 5. Rock mass strengths of G1 and D1 were higher than 20.0 MPa and that of G2 was 10.6 MPa, which was almost half of

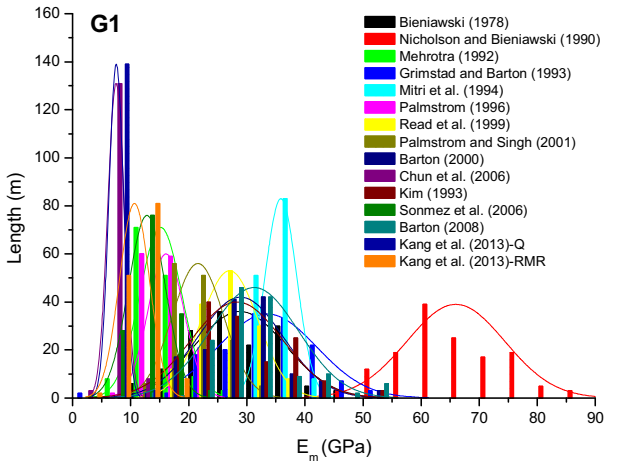

Fig. 9 **a** Histograms and normal distribution *curves* of deformation modulus for the rock unit G1; calculated from relationships in Table 5. **b** Histograms and normal distribution *curves* of deformation modulus for the rock unit G1; calculated from relationships selected for the study

G1. The rock mass strength of G3 and D3 was approximately 5.5 MPa, but that of F3 was 3.2 MPa. The RMi, also representing rock mass strength, was quite different from that estimated by the empirical relationships. The RMi values of the rock units were smaller than the rock mass strengths calculated from the relationships, except for the rock mass strength of D1, whose RMi was higher than the calculated strength.

Cohesion and friction angle

The cohesion and friction angle of the rock mass represents the ability of the rock mass to withstand shear stress (Schellart 2000). Five relationships were suggested

Table 3 Deformation modulus E_m (GPa) calculated from empirical relationships

Rock unit	G1	G2	G3	D1	D3	F3
Mean	28.5	16.1	9.80	30.4	7.40	5.00
St dev	7.90	7.40	5.00	10.7	5.70	3.40
Max	53.0	43.9	20.5	50.5	23.7	12.5
Min	3.10	0.10	2.00	0.60	2.50	1.00
CV	28 %	46 %	51 %	35 %	77 %	69 %

(Table 6). Most relationships used RMR, but Barton (2008) used J_r, J_a, and J_w to calculate a friction angle. The relationships proposed by Trueman (1988) and Kim (1993) were chosen to predict cohesion, whereas those suggested by Trueman (1988) and Bieniawski (1989) were used to determine friction angle. Table 7 shows the results of the rock units. Similar to the deformation modulus and the compressive strength, G1 and D1 had the highest mean cohesion and friction angle, while the lowest values were estimated for F3.

Rock mechanical site-descriptive model (RMSDM)

A three-dimensional block model that covers the domain of the KURT-2 was developed by combining the same rock units along three boreholes in Fig. 5. The block size was 85 m × 120 m × 80 m, and the distribution of six units at three surfaces of the block is also shown in Fig. 10a. G1 with the best rock quality in the block occupied most of the volume. G2 was distributed at the central portion of the block as a band with uneven width and almost vertical dip. The maximum width was approximately 15.5 m, and the minimum width was less than 0.5 m. G3 appeared in the left corner of the block as a small area, but the volume increased as the elevation drops. The width of G3 at the top surface was 7.0–9.0 m. Two pairs of D1 were distributed at the center and right side of the block. D1 distributed at the center of the block was very narrow and 0.5 m in thickness. However, D1 at the right side of the block was much wider than the other. D3 was as narrow as D1, at the same time, parallel to the adjacent D1. Dips of D1 and D3 were almost vertical. F3 was clearly visible as a narrow band, and the orientation of F3 was in N3E and 63SE.

The block diagram was cut at the elevation of the KURT-2 excavation, and the two-dimensional rock unit distributions are shown in Fig. 10b. All six rock units were identified in the area, but the G1 and G2 units dominated. F3 crossed the area in north–south direction. Since the tunnel for KURT-2 had been completely excavated and face-mapping data of the tunnel became available, rock mass distributions from the modeling

Table 4 Suggested empirical equations to estimate rock mass strength σ_m

Empirical equation	Required parameters	Equations
Hoek and Brown (1980)	RMR, σ_{ci}	$\sigma_m = \sigma_{ci} e^{(RMR - 100)/18}$
Yudhbir et al. (1983)	RMR	$\sigma_m = e^{7.65(RMR - 100)/100}$
Ramamurthy (1986)	RMR, σ_{ci}	$\sigma_m = \sigma_{ci} e^{(RMR - 100)/18.75}$
Singh and Singh (1993)	q_c	$\sigma_m = 5rq_c^{1/3}$
Kalamaris and Bieniawski (1995)	RMR, σ_{ci}	$\sigma_m = \sigma_{ci} e^{(RMR - 100)/24}$
Sheorey (1997)	RMR, σ_{ci}	$\sigma_m = \sigma_{ci} e^{(RMR - 100)/20}$
Singh et al. (1997)	Q	$\sigma_m = 0.38rQ^{1/3}$
Aydan and Dalgic (1998)	RMR, σ_{ci}	$\sigma_m = \sigma_{ci}^{RMR/[RMR + 6(100 - RMR)]}$
Trueman (1988)	RMR	$\sigma_m = 0.5e^{(0.6RMR)}$
Barton (2000)	Q, σ_{ci}	$\sigma_m = \gamma(Q \times \sigma_{ci}/100)^{1/3}$

σ_{ci}, q_c UCS of intact rock, γ unit weight of rock mass

Table 5 Rock mass strength σ_m (MPa) calculated from relationships

	Rock unit	G1	G2	G3	D1	D3	F3
From empirical relationships	Mean	22.2	10.6	5.50	27.7	4.90	3.2
	St dev	8.50	5.10	2.50	15.2	3.90	2.2
	Max	50.4	30.9	10.7	68.3	13.5	8.9
	Min	6.90	1.00	0.80	10.0	0.70	0.3
	CV	38 %	48 %	45 %	55 %	80 %	70 %
RMi values	Mean	17.7	5.80	3.70	33.6	2.20	0.5
	St dev	9.80	4.30	3.10	14.5	2.20	0.7
	Max	45.2	23.1	9.00	48.8	5.00	1.5
	Min	1.70	1.30	0.10	5.80	0.80	0.1
	CV	55 %	74 %	82 %	43 %	101 %	139 %

Table 6 List of relationships to estimate cohesion (c_m) and friction angle (ϕ_m)

Empirical equations	Required parameters	Equations
Trueman (1988)	RMR	$c_m = 0.25e^{(0.05RMR)}$
		$\phi_m = 0.5RMR + 5$
Bieniawski (1989)	RMR	$c_m = -0.051 + 0.008RMR - (3.46 \times 10^{-5})RMR^2$
		$\phi_m = -0.086 + 0.7891RMR - 0.0031RMR^2$
Kim (1993)	RMR	$c_m = 2e^{(0.08RMR)}$
		$\phi_m = 0.25RMR + 27.5$
Aydan and Kawamoto (2000)	RMR	$\phi_m = 20 + 0.05RMR$
Barton (2008)	J_r, J_a, J_w	$\phi_m = \frac{1}{1.124}\tan^{-1}\left(\frac{J_r}{J_a} \times J_w\right)$

J_r joint roughness number, J_a joint alteration number, J_w joint water reduction factor

results and face mapping are given in Fig. 10b and c. The finding was that predicted distributions were similar to those observed. However, G2 occupied a larger area than predicted one, and D1, a thin dike, was not visible. The area where G3 was identified was quite different. Such differences might be caused by a scaling effect. The predicted distributions were based on the observations from small cores, but the area observed from face

Table 7 Cohesion c_m (MPa) and friction angles φ_m (°) calculated from relationships

Rock unit	G1		G2		G3		D1		D3		F3	
	c_m	ϕ_m	c_m	ϕ_m	c_m	ϕ_m	c_m	ϕ_m	c_m	ϕ_m	c_m	ϕ_m
Mean	5.0	37.5	2.5	32.0	1.5	27.5	4.4	36.3	1.1	25.6	0.9	22.2
St dev	1.9	1.80	1.4	2.90	0.9	3.20	2.3	3.40	0.8	2.10	0.8	5.50
Max	9.8	41.7	6.6	38.3	3.1	31.8	8.7	40.6	2.4	29.1	2.8	30.6
Min	0.3	33.2	0.5	25.3	0.3	21.7	1.1	30.1	0.4	23.6	0.1	15.5
CV	37 %	5 %	55 %	9 %	65 %	12 %	52 %	10 %	71 %	8 %	90 %	25 %

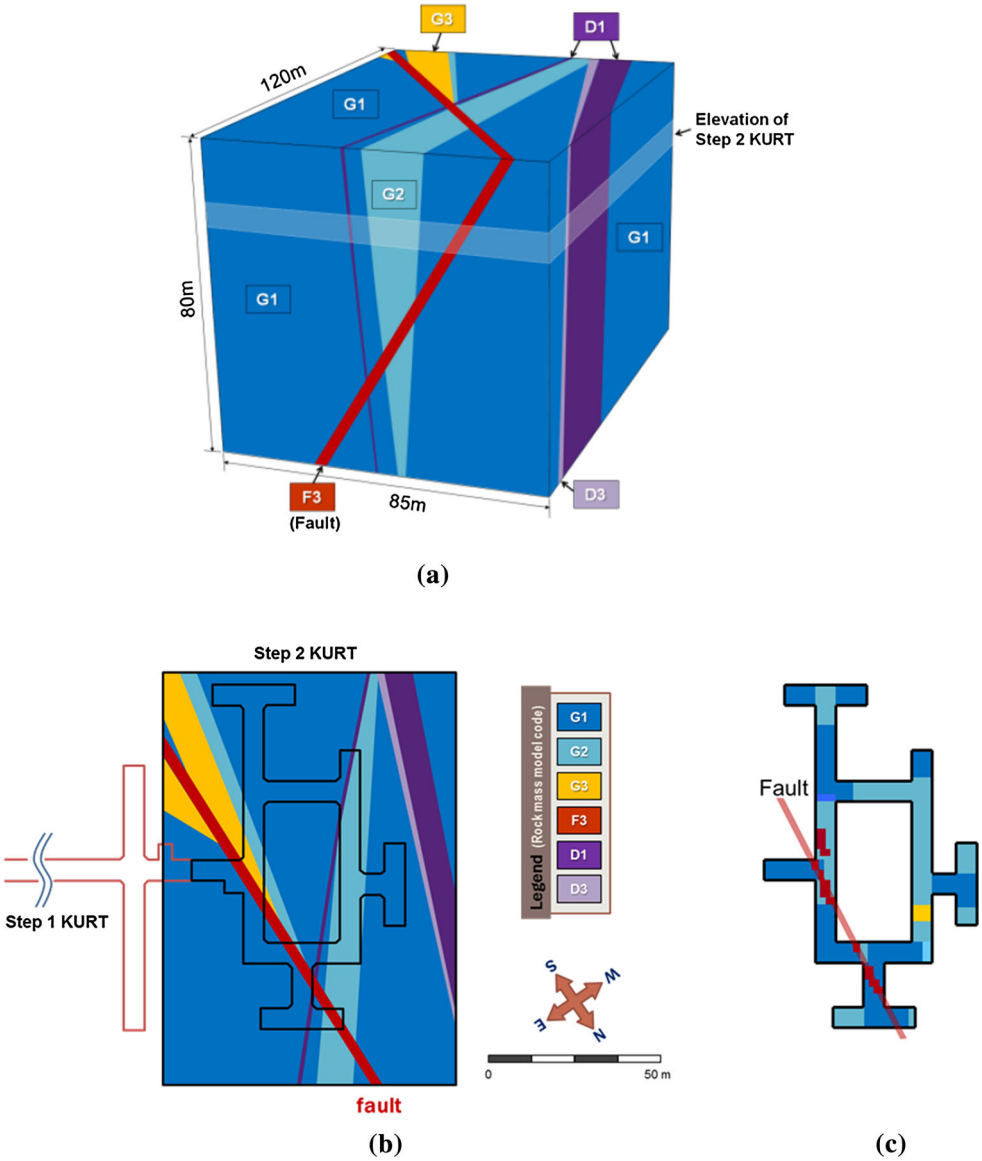

Fig. 10 **a** Three-dimensional block model covering KURT-2 domain. Two-dimensional distributions of rock units at the elevations of KURT-2 excavation from **b** modeling, and **c** face mapping after excavation

mapping was much larger than the cores. The qualities and mechanical properties of rock mass are summarized in Table 8. G1 and D1 were the best rock mass in this domain, having similar qualities and mechanical properties. The quality and properties of G2 were in medium class. G3 and D3 were similar but poor, and F3 had the poorest quality and lowest mechanical properties in this domain.

Table 8 Mechanical properties of rock mass for each rock unit

Rock unit	G1	G2	G3	D1	D3	F3
Q	28.4	9.80	3.00	34.3	2.10	0.10
RMR	64.1	52.5	43.5	61.8	39.7	29.7
RMi (MPa)	17.7	5.80	3.70	33.6	2.20	0.50
E_m (GPa)	28.5	16.1	9.80	30.4	7.40	5.00
σ_m (MPa)	21.4	9.60	5.20	28.9	4.50	2.80
c_m (MPa)	5.00	2.50	1.50	4.40	1.10	0.90
φ_m (°)	37.5	32.0	27.5	36.3	25.6	22.2

Conclusions

KAERI has just completed the construction of the second stage of KURT (KURT-2) to execute future research on the safe disposal of SNF waste in Korea. A site investigation was successfully conducted to characterize rock mass in KURT-2, and developed an RMSDM. At the tunnel excavation sites, rock mass qualities (rock types and fracture developments) and Q and RMR values were visualized in terms of the RMSDM. Therefore, rock mass qualities and mechanical properties of rock mass determined by the developed RMSDM could be utilized as a basis for supporting engineering design and stability analysis, and may technically contribute to several tests and experiments for the future KAERI research and development (R&D) projects.

Acknowledgments This study was supported by the National Nuclear Research and Development Program through the National Research Foundation, funded by The Ministry of Science ICT & Future Planning of Korea (NRF-2012M2A8A5025579).

References

Andersson J, Christiansson R, Hudson J (2002) Site investigations: strategy for rock mechanics site descriptive model. Swedish Nuclear Fuel and Waste Management Co, Technical Report TR-02-01, p 155

Andersson J, Skagius K, Winberg A, Lindborg T, Strom A (2013) Site-descriptive modelling for final repository for spent nuclear fuel in Sweden. Environ Earth Sci 69:1045–1060

Aydan O, Dalgic S (1998) Prediction of deformation behavior of 3-lanes Bolu tunnels through squeezing rocks of North Anatolian fault zone (NAFZ). Proceedings Regional Symposium on sedimentary rock engineering, Taipei, Taiwan, pp 228–233

Aydan O, Kawamoto T (2000) The assessment of mechanical properties of rock masses through RMR rock classification system. Proceedings ISRM International Symposium. International Society for Rock Mechanics, Melbourne, Australia, UW0926 (on CD)

Barton N (1988) Rock mass classification and tunnel reinforcement selection using the Q-system. In: Kirkaldie L (ed) Rock classification systems for engineering purposes, ASTM STP 984. American Society for Testing Materials, Philadelphia, pp 59–88

Barton N (2000) TBM tunnelling in jointed and faulted rock. CRC Press, p 184

Barton N (2008) Training course on rock engineering. Organized by ISRMTT & CSMRS, Course Coordinator Rajbal Singh, December 10–12, New Delhi, p. 502

Barton N, Lien R, Lunde J (1974) Engineering classification of rock masses for the design of tunnel support. Rock Mech 6:189–236

Bieniawski ZT (1973) Engineering classification of jointed rock masses. Transf S Afr Inst Civ Eng 15:335–344

Bieniawski ZT (1976) Rock mass classification in rock engineering. In: Bieniawski ZT (ed) Exploration for Rock Engineering. AA Balkema, Cape Town, pp 97–106

Bieniawski ZT (1978) Determining rock mass deformability experience from case histories. Int J Rock Mech Min Sci 15(5):237–247

Bieniawski ZT (1989) Engineering rock mass classifications. Wiley, New York, p 251

Brantberger M, Zetterqvist A, Arnbjerg-Nielsen T, Olsson T, Outters N, Syrjanen P (2006) Final repository for spent nuclear fuel. Underground design Forsmark, Layout D1. SKB R-06-34

Bredehoeft J (2005) The conceptualization model problem-surprise. Hydrogeol J 13:37–46

Cho WJ, Kwon SK, Park JH (2008) KURT, a small-scale underground research laboratory for the research on a high-level waste disposal. Ann Nucl Energy 35:132–140

Chun BS, Lee YJ, Jung SH (2006b) The evaluation for estimation method of deformation modulus of rock mass using RMR system. Korean Geoenviron Soc 7:25–32

Deere DU (1968) Geological considerations. In: Stagg RG, Zienkiewics DC (eds) Rock mechanics in engineering practice. Wiley, New York, pp 1–20

Fälth B, Hökmark H (2006) Seismically induced slip on rock fractures. Results from dynamic discrete fracture modeling. SKB R-06-48, Swedish Nuclear Fuel and Waste Management Co, Stockholm

Glamheden R, Fredriksson A, Röshoff K, Karlsson J, Hakami H, Christiansson R (2007) Rock mechanics Forsmark site descriptive modeling, Forsmark stage 2.2. SKB R-07-31, Swedish Nuclear Fuel and Waste Management Co, Stockholm

Grimstad E, Barton N (1993) Updating the Q-system for NMT. Proceedings International Symposium On Sprayed Concrete. Fegernes, Norwegian Concrete Association, Tapis Press, Trondheim, pp 46–66

Hakami E, Hakami H, Cosgrove J (2002) Strategy for rock mechanics site descriptive model, development and testing of an approach to modelling the state of stress. SKB R-02-03, Swedish Nuclear Fuel and Waste Management Co, Stockholm

Hashemi M, Moghaddas SH, Ajalloeian R (2010) Application of rock mass characterization for determining the mechanical properties of rock mass: a comparative study. Rock Mech Rock Eng 43:305–320

Hoek E (1994) Strength of rock and rock masses. ISRM News J 2(2):4–16

Hoek E, Brown ET (1980) Underground excavations in rock. Institution of Mining and Metallurgy, London, p 527

Hoek E, Kaiser PK, Bawden WF (1995) Support of underground excavations in hard rock. AA Balkema, Rotterdam, p 215

Holland KL, Lorig LJ (1997) Numerical examination of empirical rock-mass classification systems. Int J Rock Mech Min Sci 34:3–4

Hudson JA (2002) Strategy for a rock mechanics site descriptive model. A test case based on data from the Äspö HRL, SKB Report R-02-04, Swedish Nuclear Fuel and Waste Management Co, Stockholm

International Society for Rock Mechanics (ISRM) (1981) Rock characterization, testing and monitoring. In: Brown ET (ed) ISRM suggested methods. Permagon Press, New York

Kalamaris GS, Bieniawski ZT (1995) A rock mass strength concept for coal incorporating the effect of time. Proceedings 8th ISRM Congress. International Society for Rock Mechanics, Chiba, Japan, pp 295–302

Kang SS, Kim HY, Jang BA (2013) Correlation of in situ modulus of deformation with degree of weathering, RMR and Q-system. Environ Earth Science 69:2671–2678

Kim GW (1993) Revaluation of 'Geomechanics classifications of rock masses'. In: KGS Spring 93 National Conference/Geotech Eng and Tunn Technol, Seoul, pp 33–40

Kim GW, Kim SJ (2006) Correlation between engineering properties of rocks in Korea. J Eng Geol 16:59–68

Kim KS, Park KW, Kim GY, Choi HJ (2012) Potential repository domain for A-KRS at KURT facility site. J Korean Radioact Waste Soc 10:151–159

Kwon S, Cho WJ (2008) The influence of an excavation damaged zone on the thermal-mechanical and hydro-mechanical behavior of an underground excavation. Eng Geol 101:110–123

Kwon S, Cho WJ (2009) A sensitivity analysis of design parameters of an underground radioactive waste repository using a back propagation neural network. Tunn Undergr Space 19:203–212

Kwon S, Park JH, Cho WJ (2004) Geotechnical characteristics of the site for an underground research tunnel in KAERI, KAERI Technical Report, KAERI/TR-2305/2004

Kwon S, Cho WJ, Han PS (2006) Concept development of an underground research tunnel for validating the Korean reference HLW disposal system. Tunn Undergr Space Technol 21:203–217

Kwon S, Lee CS, Cho SJ, Jeon SW, Cho WJ (2009) Investigation of excavation damaged zone at KAERI underground research tunnel. Tunn Undergr Space Technol 24:1–13

Makurat A, Löset F, Wold Hagen A, Tunbridge L, Kveldsvik V, Grimstad E (2006) Äspö HRL A descriptive rock mechanics model for the 380–500 m level. Norwegian Geotechnical Institute, Oslo, Swedish Nuclear Fuel and Waste Management Co, SKB R-02-11, p 179

Mehrotra VK (1992) Estimation of engineering parameters of rock mass. PhD Thesis, University of Roorkee, India

Mitri HS, Edrissi R, Henning J (1994) Finite element modeling of cable-bolted slopes in hard rock underground mines. SME Annual Meeting, February 14–17, New Mexico SME, Albuquerque, pp 94–116

Nicholson GA, Bieniawski ZT (1990) A nonlinear deformation modulus based on rock mass classification. Int J Min Geol Eng 8(3):81–202

Nordstrom DK (2012) Models, validation, and applied geochemistry: issues in science, communication, and philosophy. Appl Geochem 27(10):1899–1919

Palmström A (1995) RMi: a rock mass classification system for rock engineering purposes. PhD Thesis, The University of Oslo

Palmström A (1996) Characterization of rock masses by the RMi for use in practical rock engineering. Tunn Undergr Space Technol 11(2):175–186

Palmström A, Singh R (2001) The deformation modulus of rock masses-comparisons between in situ tests and indirect estimates. Tunn Undergr Space Technol 16(3):115–131

Ramamurthy T (1986) Stability of rock mass. 8th Annual lecture, Indian Geotech J, pp 1–74

Ramamurthy T, Arora VK (1993) A Classification for intact and jointed rocks. In: Anagnostopoulos A, Frank R and Kalteziotis N (eds) Geotechnical engineering of hard soils-soft rocks. Taylor and Francis, Rotterdam, pp 235–242. ISBN: 10: 9054103442

Read SAL, Richards LR, Perrin ND (1999) Applicability of the Hoek-Brown failure criterion to New Zealand greywacke rocks. Proceedings 9th International Soc Rock Mech Congress Paris, vol 2, pp 655–660

Rönkkönen H, Hakala M, Paananen M, Laine E (2012) ONKALO rock mechanics model (RMM)-version 2.0, POSIVA Working Report 2012–07, p 94

Schellart WP (2000) Shear test results for cohesion and friction coefficients for different granular materials: scaling implications for their usage in analogue modeling. Tectonophysics 324:1–16

Sheorey PR (1997) Empirical rock failure criterion. Balkma, Rotterdam

Singh VK, Singh DP (1993) Correlation between point load index and compressive strength for quartzite rocks. Geotech Geol Eng 11:269–272

Singh B, Goel RK (2011) Engineering rock mass classification: tunneling, foundations and landslides. Butterworth-Heinemann, Oxford

Singh B, Viladkar MN, Samadhiya NK, Mehrota VK (1997) Rock mass strength parameters mobilized in tunnels. Tunn Undergr Space Technol 12:47–54

SKB (2000) Geoscientific programme for investigation and evaluation of sites for the deep repository. SKB TR-00-20, Swedish Nuclear Fuel and Waste Management Co, Stockholm, p 115

SKB (2001) Site investigations. Investigation methods and general execution programme. SKB TR-01-29, Swedish Nuclear Fuel and Waste Management Co, Stockholm

SKB (2002) Forsmark-site descriptive model version 0. SKB R-02-32, Swedish Nuclear Fuel and Waste Management Co, Stockholm

Sonmez H, Gokceoglu HA, Nefeslioglu A, Kayabasi A (2006) Estimation of rock modulus: for intact rocks with an artificial neural network and for rock masses with a new empirical equation. Int J Rock Mech Min Sci 43:224–235

Staub I, Fredriksson A, Outters N (2002) Strategy for a rock mechanics site descriptive model. Development and testing of the theoretical approach, R-02-02, Swedish Nuclear Fuel and Waste Management Co., Sweden, p 219

Terzaghi K (1946) Rock defects and load on tunnel supports. In: Proctor RV, White TL (eds) Introduction to rock tunneling with steel supports. Commercial Sheering & Stamping Co, Youngstown

Trueman R (1988) An evaluation of strata support techniques in dual life gateroads. PhD Thesis, University of Wales Cardiff, pp 81–102

Yudhbir Y, Lemanza W, Prinzl F (1983) An empirical failure criterion for rock masses. Proceedings 5th ISRM Congress. International Society for Rock Mechanics, Melbourne, Australia, 1B, pp 1–8

Zhang LY, Einstein HH (2004) Using RQD to estimate the deformation modulus of rock masses. Int J Rock Mech Min Sci 41:337–341